Stability of water-level controls in hydropower plants accounting for backlash, delays and instrumental errors

Stability of water-level controls in hydropower plants accounting for backlash, delays, and instrumental errors

Riccardo Vesipa, Alejandro Marmolejo Gutierrez, Luca Ridolfi
Politecnico di Torino (Italy)

ABSTRACT
We discuss the stability of run-of-river (ROR) hydropower plants. Despite this problem has been tackled for a long time, the relevant literature usually disregards important mechanisms such as: (i) backlash in mechanical actuators and components, (ii) delays in data processing and transmission, (iii) measurement uncertainties occurring in sensors, (iv) finite velocity of actuators, and (v) pressure surges within the penstock and in the head-race tunnel. The aim of this paper is to show the relevance of these (nonlinear) mechanisms on the stability of water-level controls in ROR plants.

1 INTRODUCTION

We discuss a classical problem of hydraulic and control engineering: the stability of run-of-river (ROR) hydropower plants. ROR hydropower plants are widely adopted worldwide [1] and represent a typical example of engineering systems that exhibit stability issues. For this reason, they have been a relevant research subject [2-6]. This problem has been mainly tackled by linear stability analyses (LSA). LSA are a key tool in this type of studies since, in most of the cases, they are simple to be implemented and correctly assess the stability properties of the controlled system, both in terms of asymptotic stability and transient responses [7]. A drawback of this type of analyses is that non-linear mechanisms and processes involving time delays and piecewise or threshold behaviours cannot be accounted for. This analytical difficulty explains why important mechanisms in controlled hydraulic systems such as backlash in mechanical actuators and components, data processing and transmission delays, level sensors measure uncertainties, finite velocity of actuators, and hydraulic transient within the penstock have seldom been considered in the stability analysis of ROR plants. The aim of this paper is to shed light on the relevance of these mechanisms in the context of the stability of water-level controls in ROR plants.

2 RUN-OF-RIVER HYDROPOWER PLANTS DESCRIPTION

2.1 Main characteristics of the plant

ROR plants (Figure 1) are made up of hydraulic and control components. Hydraulic components usually consist of a river uptake that feeds a forebay. The forebay is connected by the head-race tunnel to the surge tank. From the surge tank, a penstock feeds the turbine(s). Control components are a level sensor (that measures the water elevation in the forebay) and a governor, that adjusts the opening of (and thus the flow rate through) the turbine(s). The governor operations are function of the water level dynamics and are usually set by a proportional-integral (PI) control algorithm which is adopted to keep the water level of the forebay at a constant value.

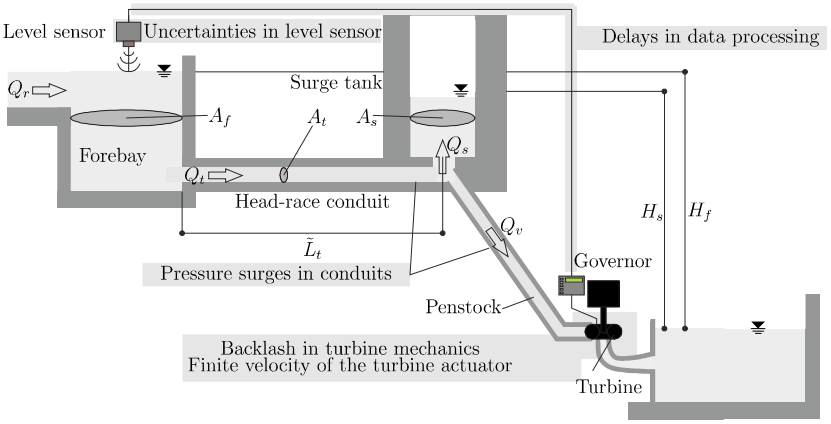

Figure 1: Schematic of a ROR plant (see text for description). Gray insets highlight the novel mechanisms here discussed.

The forebay diverts the flow rate Q_r from the river, and is characterized by a cross-section area A_f and a head H_f. The surge tank has a cross-section area A_s, and a head H_s. The flow in/out of the surge tank is Q_s. The forebay and the surge tank are connected by a head-race conduit of length L_t and cross section A_t. Downstream the surge tank, the penstock (cross section A_p) connects the turbine. The head-race conduit conveys the flow rate Q_t. In the final section of the penstock (flow rate Q_p), a turbine equipped with a governor regulates the flow rate, so that the flow rate through the turbine and in the penstock is Q_v.

The governor can adjust the relative opening of the turbine, X. Values $X = 0$ and $X = 1$ mean that the turbine is fully closed or it is at nominal opening, respectively. The relative opening can be $X>1$ when the flow rate is larger than the rated flow rate. The limit Q_{max} is the maximum flow attained in the penstock when the turbine is fully open. An algorithm implemented in the valve PLC (Programmable Logic Controller) determines the relative opening of the valve, X. The aim of valve-regulation algorithms is to set X, as a function of the dynamics of the water level in the forebay. The water level in the forebay, H_f, is measured by a sensor that sends the signal to the turbine programmable-logic-controller (PLC). The algorithm implemented in the PLC compares H_f to a target value, H_{trg}. Regulation is performed to keep H_f as close to H_{trg} as possible. To this aim, a PI (proportional-integral) control algorithm is usually adopted [2-6].

2.2 Error sources in the level control system

In the level control system, some undesired mechanisms affect the dynamics of the turbine opening X. They are: uncertainties in level sensors, delays in data treatment, backlash, and finite velocity in turbine's mechanics. These mechanisms cause the actual opening of the turbine X to be different from the optimal opening of the turbine X set by an ideal control system.

In the previous section, it was highlighted that the dynamics of the system strongly depends on the measurement of the water level of the forebay. However, true value $H_{f,true}$ is never known. Instead, it is only possible to determine a measured value $H_{f,meas}$, that – due to measurement errors - departs from the true value.

In the context of this work, delays are defined as the interval of time taken by the control system from the measure of the water level in the forebay to the activation of the actuator. This time interval is referred as delay since control operations are not performed exactly at the time the forebay level is measured.

Backlash (see inset in Figure 1) is a clearance or loss of motion in a mechanism due to gaps between the parts or insufficient torque due to friction [8]. Considering backlash in control systems is an important issue because it prevents an operation requested by the controller to be completely performed.

It should also be noted that the actuator needs some time to modify the opening of the valve X. If the actuator has an infinite velocity, any opening adjustment ΔX set by the PLC can be instantaneously achieved. This is not the case, because the actuator does have a finite velocity.

3 MATHEMATICAL MODEL AND NUMERICAL METHODS

3.1 Model

3.1.1 Hydraulics

Hydraulics in the conduits (penstock and head-race tunnel) is modelled through the dynamic and the continuity equations suitable for studying pressure surges [9]

$$\frac{\partial Q}{\partial t} + gA\frac{\partial H}{\partial x} + \frac{f}{2DA}Q|Q| = 0\,, \qquad \frac{a^2}{gA}\frac{\partial Q}{\partial x} + \frac{\partial H}{\partial t} = 0\,, \tag{1a,b}$$

where Q=flow rate, H=pressure head, t=time, x=spatial coordinate along the conduit (x=0 is the upstream end, x=L is the downstream end, where L is the length of the conduit). The other symbols stand for: g = gravity acceleration, D = diameter of the conduit, A = cross-section of the conduit, f = friction factor according to the Darcy-Weisbach formula and a = wave speed in the conduit. The subscripts "t" and "p" were used to refer to the head-race tunnel and the penstock, respectively.

Boundary conditions for the forebay, surge tank, and downstream valve are implemented according to [9]. In the forebay, the flow $Q_t(t, x_t=0)$ enters the head-race tunnel. The head $H_t(t, x_t=0)$ at the entrance of the tunnel can be computed as

$$H_t\left(t, x_t = 0\right) = H_f\left(t\right) - (1 + k_e)\frac{\left(Q_t(t, x_t = 0)\right)^2}{2gA_t^{\,2}}\,,$$
$$\frac{dH_f(t)}{dt} = \frac{Q_r(t) - Q_t(t, x_t = 0)}{A_f}\,, \tag{2a,b}$$

where k_e = 0.5 = coefficient of entrance loss. The water level in the forebay varies over the time according to the mass balance equation (2b). This equation states that the forebay level changes over time when the flow entering the head-race tunnel $Q_t(t, x_t=0)$ and the flow taken from the river $Q_r(t)$ are different.

In the surge tank, the head losses are usually neglected. It follows that the head in the node in which the tunnel, the penstock and the surge tank converge is given by (3a). The water level in the surge tank varies over the time according to the mass balance equation (3b)

$$H_t\left(t, x_t = L_t\right) = H_p\left(t, x_p = 0\right) = H_s(t)\,, \quad \frac{dH_s\left(t\right)}{dt} = \frac{1}{A_s} Q_s\left(t\right)\,, \tag{3a,b}$$

where Q_s = flowrate in the surge tank. This flow is defined as positive if it enters the surge tank, and is given by the continuity equation $Q_s\left(t\right) = Q_t(t, x_t = L_t) - Q_p(t, x_p = 0)$.

The downstream turbine is modelled as a flow through an orifice [9]. Considering the datum at the free surface of the tailrace (approximately equal to the level of the turbine), the discharge flowing through the needle valve is described by the equation

$$Q_v\left(t\right) = A_v\left(t\right) c_v \sqrt{2 g H_v\left(t\right)}\,, \tag{4}$$

where the head at the valve is taken as the head at the end of the penstock, i.e., $H_v(t) = H_p(t, x_p = L_p)$. The opening of the valve varies through time and is determined by equations (5a,b) described in the following subsection.

3.1.2 Controls

The turbine opening $A_V(t)$ is regulated by the PI controller. In this control, the level in the forebay $H_f(t)$ is measured and compared with a target value. If the measured level is different from the target value, the turbine opening is modified using the equation [2]

$$\frac{dX(t)}{dt} = \frac{H_f\left(t\right) - H_{\text{trg}}}{T_i} + k \frac{d(H_f\left(t\right) - H_{\text{trg}})}{dt}\,,\ X\left(t\right) = \frac{A_v(t)}{A_{rated}}\,. \tag{5a,b}$$

where the subscript “rated" means “rated value”, while T_i and k are the integral and proportional constants of the PI controller, defined as

$$T_i = \frac{L_t\, Q_{rated} H_{\text{trg}}}{K_1\, g\, H_{s,rated}\, A_t}\,,\ k = \frac{\alpha}{H_{\text{trg}}}\,, \tag{6a,b}$$

where α and K_1 are parameters of the PI controller. The integration over a finite time Δt of (5a) gives the turbine opening adjustment ΔX.

3.1.3 Error mechanisms in the level control system

In an ideal situation, no sensor uncertainties, errors, or delays affect the control system. This means that: (i) the exact value of forebay level $H_f(t)$ is known; (ii) the PI algorithm (5a,b) can instantaneously determine the adjustment of the turbine opening ΔX; (iii) this adjustment is performed instantaneously, and (iv) no mechanical issues exist, and the new opening adjustment prescribed by the algorithms, ΔX is attained by the actuator with a perfect precision. This is not the case because sensor uncertainties, electronic delays, and mechanical issues occur. As a result of all these mechanisms, the opening adjustment of the turbine attained is different from the opening adjustment of the turbine that an ideal control system would have attained. Now, we describe how all these error mechanisms have been modelled in this work.

Level sensor uncertainties can be accounted for in the mathematical model by considering the measured value H_{meas} as a random extraction from a population of measures described

by a probability distribution function. In the present study, the Standard Normal Distribution is used. It reads [10]

$$\varphi(Z) = e^{-\frac{Z^2}{2}} \Big/ \sqrt{2\pi} \,, \tag{7}$$

where $Z=(H_{f,meas}-H_f)/\sigma_{Hf}$ is the standardized normal random variable and σ_{Hf} is the standard deviation of the forebay level. In this work, uncertainties are applied to the forebay level as follows: the true water level in the forebay H_f is modelled through the deterministic equations (1-4). Then, a population of possible measurement - centred around the modelled value H_f - is built according to (7), and a random extraction of a measurement is performed. This extraction gives the measured value $H_{f,meas}$. This value is used by the level controller as an input, and it is thus used in place of H_f in (5a) to determine the turbine opening adjustment.

The delay in the system is considered assuming that the operation performed by the actuator is carried out t_{delay} seconds after the measure in the forebay. In this work, delays occurring in signal treatment are applied as follows: when the adjustment opening ΔX is evaluated, the new turbine opening $A_v(t)$ is not implemented in (4) until t_{delay} seconds have passed.

Backlash is modelled in terms of gaps between mechanical parts and friction losses. The gaps G_+ and G_- are modelled as a percentage of the rated area [11], namely

$$G_+(t) = \frac{\Delta A_{v,open}(t)}{A_{v,rated}}, G_-(t) = -\frac{\Delta A_{v,close}(t)}{A_{v,rated}}, \tag{8a,b}$$

where $\Delta A_{v,open}(t)$ (or $\Delta A_{v,close}(t)$) is the time-dependent valve opening which is lost due to gaps between mechanical parts when the actuator drives in the opening (or closing) direction (see Figure 2a). If the actuator starts from a neutral position (see Figure 2b), the gaps occurring in the opening and closing direction are $G_{+,\max}$ and $G_{-,\max}$, so the total gap that occurs when the actuator reverses direction is

$$G_{total} = G_{+,\max} + \left| G_{-,\max} \right| . \tag{9}$$

Friction losses are considered by setting a parameter μ that quantifies the percentage of valve opening that is lost due to frictional forces. From μ follows the parameter $b=1-\mu$.

Starting from these definitions, it is possible to estimate the actual change of valve opening ΔX_{real} that is attained over the time Δt when the PI controller imposes a valve opening adjustment ΔX. Because of gaps between mechanical parts and friction forces, ΔX_{real} is always lower than ΔX. From a quantitative point of view, focusing on an increment of turbine opening, ΔX_{real} can be modelled as

$$\text{if } \Delta X < G_+ \rightarrow \Delta X_{real} = 0; \quad \text{if } \Delta X > G_+ \rightarrow \Delta X_{real} = (dX - G_+) \cdot b \,. \tag{10a,b}$$

The first equation (10a) states that if the prescribed adjustment ΔX is lower than the minimum prescribed adjustment for which all gaps between mechanical parts are closed (MPA henceforth), no opening adjustment takes place (arrow A in Figure 2b). The second equation (10b) holds when the prescribed adjustment ΔX is larger than MPA. In this case, the real adjustment ΔX_{real} is larger than zero, but lower than the prescribed adjustment ΔX, because of the occurrence of gaps (if any left) and friction forces within the actuator (arrow B in Figure 2b). It should be noted that the gaps between mechanical parts evolve over time according to the rules

$$\text{if } \Delta X < G_+(t) \rightarrow G_+(t+\Delta t) = G_+(t) - \Delta X; \quad \text{if } \Delta X > G_+(t) \rightarrow G_+(t+\Delta t) = 0 \,. \tag{11a,b}$$

Equation (11a) states that if (over the time interval Δt) the prescribed adjustment is lower than the MPA, the MPA at the following time ($t+\Delta t$) is reduced (arrow C in Figure 2b).

The second equation (11b) states that if the prescribed adjustment is higher than the MPA, all the gaps are closed (all mechanical parts are in contact) and remain closed until the direction of motion is reversed (arrow D in Figure 2b). Motion in the opposite direction is modelled in the same way, and leads to the schematic representation of backlash motion reported in Figure 2b.

In this work, backlash is applied as follows: the PI algorithm prescribes a turbine opening adjustment ΔX (5a), then, this turbine adjustment is put in (10) and the real turbine opening attained after the occurrence of backlash X_{real} is obtained. From ΔX_{real}, the new turbine opening X is obtained, and $X(t)$ is then used in (5b) to compute the turbine opening $A_v(t)$. Gaps are updated at each time step according to (11).

In order to take into account the finite velocity of the actuator, it is considered that the turbine opening has a finite maximum rate of change $[dX/dt]_{max,}$ expressed as %/s, i.e., percentual variation of opening occurring over one second. In other words, a limit of the value of the time derivative of X reported in (5a) is set.

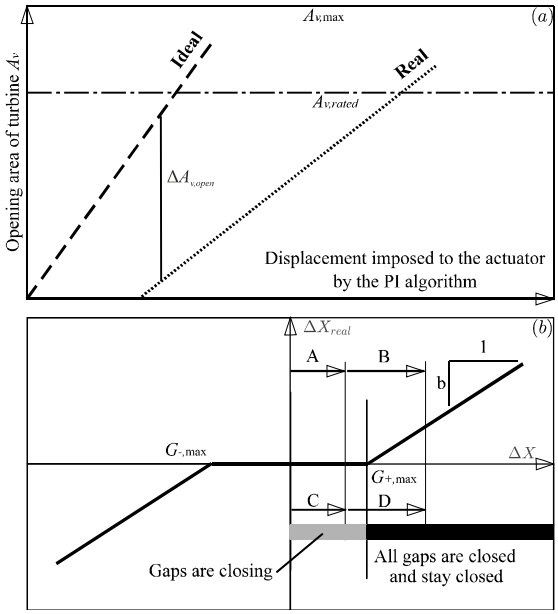

Figure 2: (a) Variation of the turbine opening A_v when the controller sets an imposed displacement (ID) to the mechanical actuator. The dashed line is the ideal behaviour, in which all the ID becomes variation of opening. The dotted line is the real behaviour, in which part of the imposed displacement is lost (gaps and friction). The dot-dashed line is the rated valve opening (i.e., X=1). For a given ID, it is possible to evaluate the lost valve opening $\Delta A_{v,open}$. (b) Schematic representation of the turbine opening adjustment in case of backlash. The real opening adjustment ΔX_{real} is always lower than the prescribed opening adjustment ΔX. It should be noted that when opening/closing goes in one direction, all gaps - at some point - are closed.

3.2 Simulation via MOC Extended-Period Analysis

To simulate the dynamics of ROR plants (considering all the mechanisms listed before) the numerical approach described in [12] and called "Extended-Period Analysis with transient models" was adopted. In short, a recursive approach is adopted according to the following steps:

(i) the MOC - as described in [9] and implemented in MATLAB scripts and routines - was applied to the whole hydraulic system, in order to solve equations (1a,b) with the boundary conditions (2a), (3a) and (4) that set turbine opening and water levels in the forebay and surge tanks. This gives the evolution of flow rates and heads from t_0 to $t_0+\Delta t$ in all computational nodes. Time steps Δt of the order of 1/100 s were used;

(ii) the flow rate at the entrance of the head-race tunnel was used to update the forebay level according to (2b); the flow rate at the end of the head-race tunnel and the flow at the entrance of the penstock were used to update the surge tank level according to (3b);

(iii) the water level in the forebay was read from the results obtained in step (ii);

(iv) measurement uncertainties occurring in the forebay water level sensor were simulated;

(v) the forebay-level time-series was given as an input to the PI algorithm aimed at keeping the level of the forebay level at a constant value by acting on the turbine opening according to (5a,b). The result of this PI algorithm is an adjustment (change of opening) of the turbine ΔX;

(vi) from the adjustment of the turbine setting given by the PI algorithm, ΔX, the backlash occurring in the turbine mechanical components and the finite velocity of the actuator were simulated and thus the actual turbine adjustment ΔX_{real} was obtained;

(vii) a delay t_{delay} was added to the operations. To do this, the actual turbine adjustment ΔX_{real} evaluated at $t_0+\Delta t$ was implemented not before the time $t_0+\Delta t+ t_{delay;}$

(viii) the change of turbine opening was implemented in the model. In this way, a new time step of the recursive numerical procedure could be started from (i) with updated forebay and surge tank levels in (2a) and (3a), and updated opening A_v in (4).

Simulations lasted up to 10 000 s. The initial conditions were set as a steady-state flow with level in the forebay H_{trg} and rated flow rate (X=1) in the plant.

4 ASSESSMENT OF SYSTEM STABILITY

A dynamical system is defined as "stable" if the small disturbances that naturally and inevitably affect the system tend to damp over time. In contrast, an unstable system exhibits an amplification of these small disturbances, that amplify to the extent of affecting the system functionality.

In the context of ROR plants, the assessment of the level-based flow controller stability is crucial. The aim of the flow control system is, in fact, to keep a constant target level H_{trg} in the forebay by adjusting the opening area of the turbine. If the flow that supplies the forebay Q_r is constant and the turbine opening, $A_{v,eq}$, is such that $Q_p(A_{v,eq})=Q_r$, then the level of the upstream tank is kept constant and no valve adjustment is required. However, this ideal configuration of equilibrium is very uncommon in real systems because, perturbations occur. The effect of these perturbations s that the flow discharged by the turbine is different from the flow entering the forebay, therefore the level of the forebay tank deviates from its target value H_{trg} and adjustments of the turbine opening are performed.

Different mathematical techniques exist to assess the response of a dynamical system to perturbations depending on the mathematical models (e.g., ODE or PDE models, autonomous or time-dependent systems), and type of perturbations (e.g., perturbation occurring only at the initial instant of the time-period, or perturbations continuously occurring throughout time). In the following, we recall two mathematical techniques that we adopted to analyse the ROR system here considered.

4.1 Linear stability analysis (LSA)

The stability of ROR plants has been traditionally tackled with the application of linear stability analyses. LSA are possible only when dynamics can be reduced to the system

$$\frac{\mathrm{d}\mathbf{Z}(t)}{\mathrm{d}t} = \mathbf{g}[\mathbf{Z}(t)], \tag{11}$$

where the vector $\mathbf{Z}(t)$ collects the dependent variables, and the N-dimensional continuous and derivable function $\mathbf{g}$ describes the system dynamics. In the theory of dynamical systems, the stability of the system is assessed studying the temporal evolution of possible perturbations of a basic state $\mathbf{Z_0}$. To discern analytically the response of a dynamical system to external disturbances, it is standard to study its linearized dynamics [13]. To this aim, the ansatz $\mathbf{Z}(t) = \mathbf{Z}_0 + \varepsilon \cdot \mathbf{z}(t)$ is introduced in (11). $\mathbf{Z_0}$ is the unperturbed basic state (i.e., $\mathrm{d}\mathbf{Z}_0 / \mathrm{d}t = \mathbf{g}[\mathbf{Z}_0] = 0$), $\mathbf{z}(t)$ are the perturbations of the basic state, and $\varepsilon<1$ is the perturbation amplitude. Taylor expansion around $\varepsilon=0$ is performed and terms of order of ε^2 or higher are disregarded. When terms of the order of ε^0 are collected, the basic state $\mathbf{Z_0}$ is obtained, whereas terms of the order ε^1 yield the linear system

$$\frac{\mathrm{d}\mathbf{z}(t)}{\mathrm{d}t} = \mathbf{A}\mathbf{z}(t), \tag{11}$$

that describes the temporal dynamics of the perturbations $\mathbf{z}(t)$. The system is deemed stable if all eigenvalues of the algebraic matrix $\mathbf{A}$ (that describes the linearized dynamics of perturbations affecting (11)) are negative. From a physical point of view, this means that all disturbances undergo an exponential decay over time. The advantage of this technique is that stability can be assessed by a simple eigenvalue evaluation and the analysis of their sign. The disadvantage is that models that involve time delays, piecewise functions, threshold behaviours cannot be considered with this approach.

4.2 Numerical simulation of the system response to perturbation

The stability properties of a dynamical system can be assessed also by numerical simulations. Examples in hydraulic engineering are provided by [7, 14-18]. In this case, numerical methods are used to simulate the evolution of a perturbation in a dynamical system at equilibrium. The perturbation can be arbitrary but should be small and physically meaningful. In order to study the stability of the water level control described in the previous sections, we studied the system response to a perturbation of the turbine opening. In details, A_v was altered of 1%, compared to $A_{v,eq}=A_{v,rated}$. Then, the behaviour of the ROR plant—initially at equilibrium, and considering all processes as described in Section 3.1.3—was simulated according to Section 3.2. Two complementary techniques were used to analyse the simulation results.

The first technique consisted in the assessment of the perturbation decay or growth rate. This was done to obtain - from numerical simulations - a result consistent and similar to those obtained from LSA, where eigenvalues are exactly the perturbation decay or growth rates. To this aim, the time-series of the forebay tank level (obtained as described in Section 4.2) are analysed. First, the perturbations of the forebay level $\gamma(t)=H_f(t)-H_{trg}$ are computed (Figure 3a,d); then, the peaks are identified (Figure 3b,e); finally, the absolute value of the peaks is evaluated, and they are fitted with the exponential curve $\Gamma=\beta \exp(\omega t)$ (Figure

3c,f). Similar to the rationale behind LSA (Section 4.1), the system is deemed as stable if $\omega<0$ (i.e., exponential decay of perturbation, panels a-c) or unstable if $\omega>0$ (panels d-f).

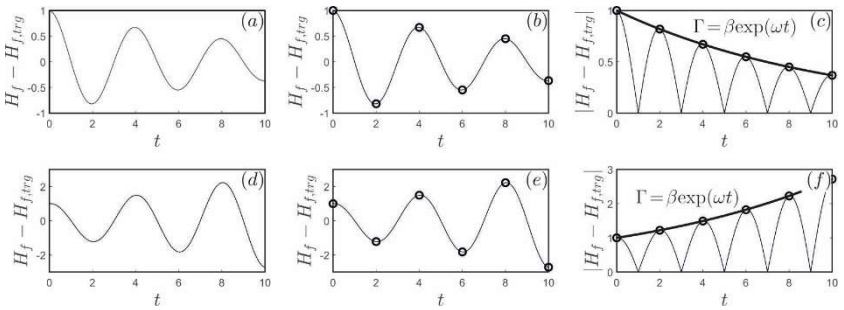

Figure 3: (a,d) Example of forebay level perturbations $\gamma(t)$; (b,e) Identification of the peaks of $\gamma(t)$; (c,f) The absolute value of the peaks of $\gamma(t)$ is evaluated, and the exponential curve $\Gamma = \beta \exp(\omega t)$ is used to fit the resulting points. The sign of ω is used to discern between stable ($\omega<1$) and unstable ($\omega>1$) cases. Panels in the first and second row report an example of stable and an unstable case, respectively.

The second technique consisted in the statistical analysis of the time-series $H_f(t)$ and $X(t)$ obtained from numerical simulations. In particular, the standard deviations σ_γ and σ_χ of the perturbation time-series $\gamma(t)=H_f(t)-H_{trg}$ and $\chi(t)=X(t)-X_{rated}$ were evaluated. This was done to quantify the amplitude of the oscillations following an initial perturbation. In order to quantify the effect of a single error mechanism, it was insightful to assess the ratio of the standard deviations $\sigma_\gamma/\sigma_{\gamma,BM}$ or $\sigma_\chi/\sigma_{\chi,BM}$, where BM stands for "benchmark case". The ratio involved a system with a single error mechanism and a benchmark case with no error mechanisms. It should be noted that in some cases the time-series $\gamma(t)$ or $\chi(t)$ approached the value "0" very quickly (e.g., left panels of Figure 5). In these cases, the standard deviation of the time-series was evaluated only over the time interval in which $\gamma(t)$ kept larger than a tolerance (±1 mm, see the dashed lines in Figure 5) around H_{target}. This introduced some arbitrariness, especially in the evaluation of $\sigma_{\gamma,BM}$ and $\sigma_{\chi,BM}$. Nevertheless, the ratios $\sigma_\gamma/\sigma_{\gamma,BM}$ or $\sigma_\chi/\sigma_{\chi,BM}$ can still provide the order of magnitude of alterations comapred to a BM case.

5 RESULTS

The main goal of this section is to discuss the effect of the different uncertainty and error mechanisms on the ROR plant controller stability. To this aim we first evaluated the system response without any of these mechanisms, finding a benchmark (BM) system response. We then repeated the analysis considering one (or more) mechanism at a time. The comparison of the BM response with the responses obtained considering additional mechanisms will allow us to quantify the effect of these mechanisms on the system stability.

5.1 Parameters adopted for the analysis

The system parameters used in the simulation are shown in Table 1. They mostly refer to the case study reported in [2]. To assess the effect of PI? parameters on the system stability, α and K_I varied in the ranges within 0-100 and 0-10, according to [2]. All the other parameters that quantify the mechanisms here considered are set to zero in the BM case. Other values are set when one (or more) mechanism at a time is considered (see the specific

sections for the adopted values). The standard formulas reported in [19] were adopted to estimate the pressure surge celerity of the head-race tunnel, a_t (circular tunnel excavated in rock) and of the penstock, a_p (circular steel pipe).

Table 1: Constant parameters used in the simulations

Variable	Symbol	Unit	Value
Forebay			
Incoming river and rated flow	Q_r	m^3/s	36.1
Surface area of the forebay	A_f	m^2	1297.3
Head target value	H_{trg}	m	112
Tunnel			
Tunnel Length	L_t	m	4005
Cross-sectional area of the tunnel	A_t	m^2	8.04
D-W Friction factor	f_t	(-)	0.009
Tunnel wave speed	a_t	m/s	1365.1
Penstock			
Penstock Length	L_p	m	276
Cross-sectional area of the penstock	A_p	m^2	8.04
D-W Friction factor	f_p	(-)	0.01
Penstock wave speed	a_p	m/s	683.5
Surge tank			
Surface area of the surge tank	A_s	m^2	61.2

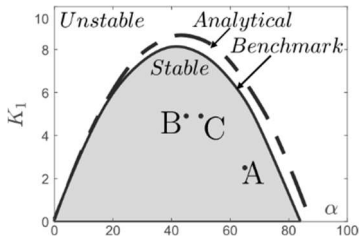

Figure 4. Bode diagram for the considered ROR plant. In the horizontal and vertical axes the PI controller parameter α and K_I are varied. The system is stable inside the curve and unstable outside. The continuous line is the marginal stability curve evaluated considering pressure surges in the conduit, and is the benchmark (BM) case of this work. The dotted line is the marginal stability curve evaluated with analytical techniques, considering a rigid column model for transients in the head-race tunnel and no transients in the penstock, as described in [2]. The parameters of Table 1 were adopted.

5.2 Effect of flow transients within the penstock and head-race tunnel

Flow transients in the conduits have negligible impact on the stability of the flow control system. In fact, the stability limit curve obtained via numerical simulations (continuous line in Figure 4) basically corresponds to the analytical curve obtained by [2] via eigenvalue analysis for a plant with the same characteristics given in Table 1 (dashed line in Figure 4): the numerical-simulation-based curve has just slightly shrunk, compared to

the analytical curve. In the following, we adopted the system behaviour obtained considering flow transients as the BM case.

5.3 Effect of uncertainties in the forebay water level sensor

Uncertainties in the forebay level sensor significantly affect the behaviour of the flow control system. Figure 5 (right panels) shows that $H_f(t)$ oscillates around H_{trg} but never converges to it throughout time. This means that, rigorously speaking, perturbations never go to zero, and is not possible to assess the system stability through the calculation of the exponential decay rate of perturbations.

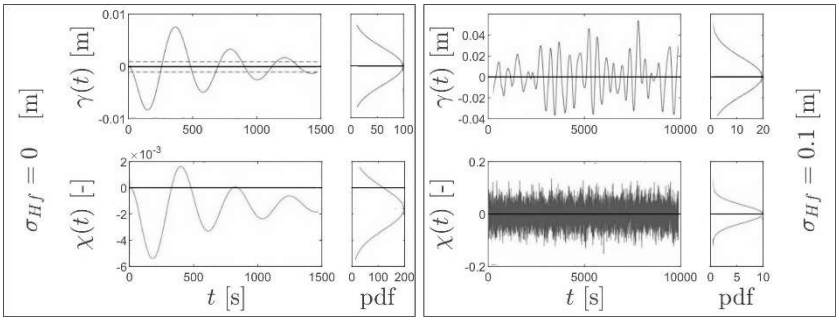

Figure 5: Each panel reports a portion of the time-series of the forebay level or turbine opening perturbation ($\gamma(t)= H_f(t)-H_{trg}$ or $\chi(t)=X(t)-X_{rated}$) and the resulting pdf of the time-series. All charts refer to Point B (α=45, K_I=5.1) in Figure 4. Panels on the left are the BM case (standard deviation of the level measure σ_{Hf}=0 m). Panels on the right were evaluated with σ_{Hf}=0.1 m.

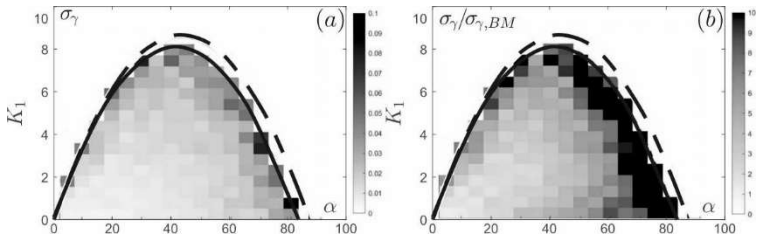

Figure 6: (a) Colormap reporting the standard deviation σ_γ of the perturbation time-series $\gamma(t)= H_f(t)-H_{trg}$ as a function of the PI controller parameters α and K_I. The darker the colour, the higher σ_γ. The marginal stability curves (continuous and dashed lines) are the same as those reported in Figure 4. Panel (b) is analogous to panel (a), except for reporting the standard deviation ratio $\sigma_\gamma/\sigma_{\gamma,BM}$ in place of σ_γ. The parameters of Table 1 and the standard deviation of the level measure σ_{Hf}=0.1 m were adopted.

In order to overcome this issue, and still get some insights, we compared the time-series of H_f and X evaluated with and without sensor uncertainties. We focused on the standard deviation of the time-series. Figure 6 shows that the standard deviation of the level in the forebay may be up 0.1 m and, more interestingly, up to 10 times greater than the oscillation occurring in a system with no uncertainties. Figure 6 also shows that these increments of oscillation amplitude are very relevant for pairs of (α, K_I) near the right boundary of the stability curve.

5.4 Effect of delays in acquisition and elaboration of signals

In order to assess the effect of delays (data acquisition and treatment) in the control systems, time lags in the range 1-30 seconds were considered. Delays of the order of the second did not show to have an important impact on the stability of the controller (Figure 7a): the behaviours of $H_f(t)$ and $X(t)$ overlapped to that of the BM case. It should be noted that delays of around 30 seconds or more (not common in modern systems) led to a system instability (Figure 7b).

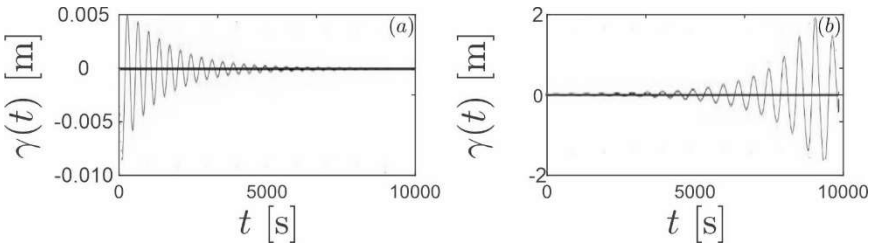

Figure 7: Portion of the time-series $\gamma(t)= H_f(t)-H_{trg}$. The charts refer to Point A (α=65, K_1=2.5) in Figure 4, and were evaluated with: (a) t_{delay}=0 s and t_{delay}=1 s (the two curves overlap perfectly), and (b) t_{delay}=30 s.

5.5 Effect of backlash

We considered maximum positive and negative gaps $G_{+,max}$ and $G_{-,max}$ equal to 0.15% and a backlash friction μ=0.005 [11]. Backlash has a significant impact on the stability of the flow control system. Similar to the case of sensor uncertainties, H_f oscillates around H_{trg} without converging to it. The amplitude of these oscillations is quite small (e.g., 0.10 m in this case reported in the right panels of Figure 8). Similar to the case of measurement uncertainties, we compare the time-series of H_f and X evaluated with and without backlash, focusing on the standard deviation of $H_f(t)$. Figure 9 shows that the standard deviation may be up 0.05 m and, up to 5 times greater than the oscillation occurring in a system with no uncertainties in level measurements. Figure 9 also shows that these increments of oscillation amplitude are very relevant for pairs of (α, K_1) near the left boundary of the stability curve.

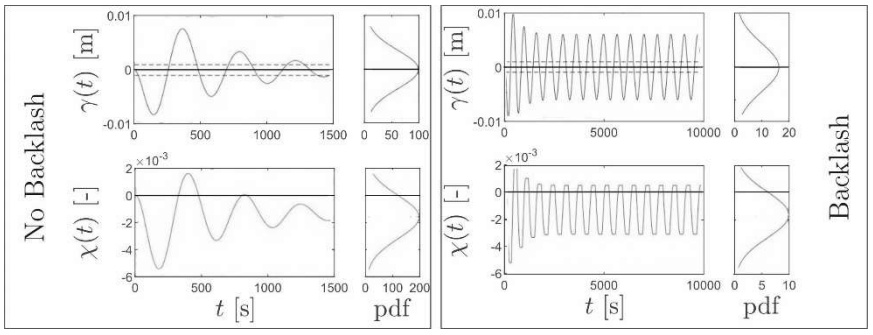

Figure 8: Each panel reports a relevant portion of the time-series of the forebay level or turbine opening perturbation ($\gamma(t)= H_f(t)-H_{trg}$ or $\chi(t)=X(t)-X_{rated}$) and the resulting pdf of the time-series. All charts refer to Point C (α=50, K_1=5) in Figure 4. Panels on the left are the BM case (No backlash). Panels on the right were evaluated with backlash.

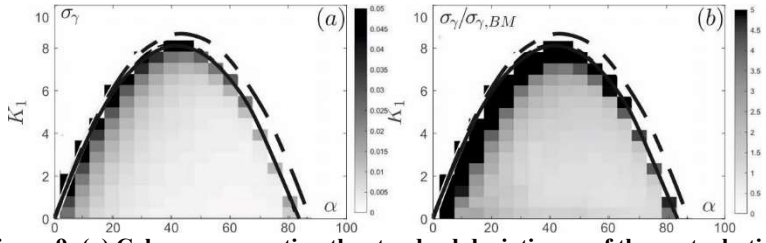

Figure 9: (a) Colormap reporting the standard deviation σ_γ of the perturbation time-series $\gamma(t)= H_f(t)-H_{trg}$ as a function of the PI controller parameters α and K_I. The darker the colour, the higher σ_γ. The marginal stability curves (continuous and dashed lines) are the same as those reported in Figure 4. Panel (b) is analogous to panel (a), except for reporting the standard deviation ratio $\sigma_\gamma/\sigma_{\gamma,BM}$ in place of σ_γ. The parameters of Table 1 and the backlash parameters $G_{+,max} = G_{-,max} = 0.15\%$ and $\mu=0.005$ were adopted.

5.6 Finite velocity of the actuator (FVA)

The finite velocity of the actuator alone did not affect the stability of the controller. The cases with FVA (evaluated with a maximum valve velocity of 2.5%/s) exhibited the same behaviour of the BM case.

5.7 Effect of combined mechanisms

No combination of two mechanisms enhanced instability, compared to the effect of single mechanism, except the combination of FVA and sensor uncertainties. For this reason, we discuss in detail this combination only.

In the previous subsections, we observed that the FVA alone has no impact in the stability, while sensor uncertainties have a moderate impact. However, the combination of these two mechanisms alters to a huge extent the system response. Physically, this behaviour occurs because when the level sensor is affected by uncertainties, significant values of ΔX (variation of valve opening) have to be implemented, to keep the water level at the target value. This was not an issue if the actuator could act with an infinite velocity, because the required ΔX could always be attained. However, when the actuator does have a finite velocity, large adjustment of valve opening, ΔX, cannot be quickly implemented. This lack of capacity of implementing the required adjustment is detrimental for the system stability. Figure 10 shows the time-series of the turbine opening and of the level in the forebay. Oscillations in the forebay level up to 2 meters and changes in the valve opening of about 40% and occurring over time-periods of few hundreds of seconds can be observed. Figure 11 demonstrates also that the behaviour reported in Figure 10 is not an isolated worst-case scenario. In fact, σ_γ is of the order of 1.5 m in a wide portion of the parameter space (α, K_I), suggesting that this type of behaviour is widespread.

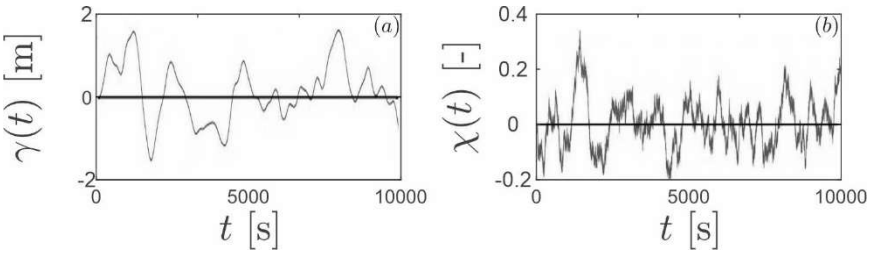

Figure 10: (a) Portion of the time-series $\gamma(t)= H_f(t)-H_{trg}$. (b) Portion of the time-series $\chi(t)=X(t)-X_{rated}$) . The charts refer to Point B (α=45, K_I=5.1) in Figure 4, and were evaluated with σ_{Hf}=0.1 m and a velocity of the actuator of 2.5%/s.

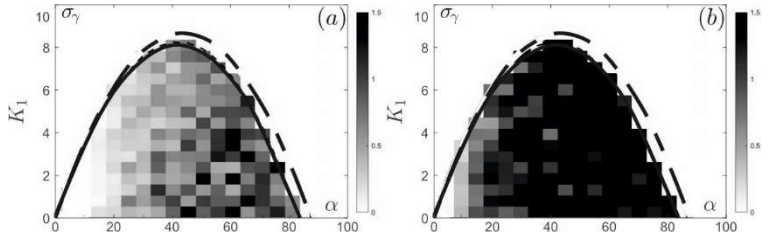

Figure 11: Colormaps reporting the standard deviation σ_γ of the perturbation time-series $\gamma(t)= H_f(t)-H_{trg}$ as a function of the PI controller parameters α and K_I. The darker the colour, the higher σ_γ. The marginal stability curves (continuous and dashed lines) are the same as those reported in Figure 4. The parameters of Table 1 and and a velocity of the actuator of 2.5%/s were adopted. Panel (a) refers to σ_{Hf}=0.05 m, whereas panel (b) refers to σ_{Hf}=0.10 m.

6 CONCLUSION

In this study, we considered a number of mechanisms previously disregarded in analysis concerning the stability of the water level control of ROR plants. Realistic parameters in terms of backlash, delays and sensor uncertainties were considered. Different mechanisms were considered both once at a time or in combination of two. We focused on a typical plant, and we found that most of the considered mechanisms (if considered alone) altered to a minor extent the system behaviour, compared to a benchmark case representative of the analysis performed so far in the literature. At most, some mechanisms (backlash, sensor uncertainties) led to a permanent state of water level and valve opening oscillations tens of time bigger than the oscillations expected in the benchmark case. Interestingly, the combination of some mechanisms (finite velocity of the turbine actuator and sensor uncertainties) led to huge and fast oscillations of water level and valve opening. It is therefore clear that a robust system of level sensors has to be implemented, as it appears to be the key to obtain system stability. One more lesson is that the other mechanism that can change, at least to some extent, the actual system response to the ideal response (benchmark case) is backlash. It is therefore advisable to invest in actuator with a reliable mechanics and, if necessary, to make use of algorithms to compensate (at least to some extent) mechanical backlash.

REFERENCES

[1] World Energy Council (2016). World Energy Resources, Hydropower.
[2] Jimenez O., Chaudhry M. (1992). Water-level control in hydropower plants. *J. Energy.Eng.-ASCE* **118**(3), pp. 180-193.
[3] Glattfelder A., Huser L. (1993). Hydropower reservoir level control - a case-study. *Automatica* **29**(5), pp. 1203-1214.
[4] Endo S., Konishi M., Imabayasi H. (2000). Water level control of small-scale hydroelectric power plant by deadbeat control method. In: *IECON 2000*: 26th Annual Conference of the IEEE Industrial Electronics Society, pp. 1123-1128.
[5] Sarasua J.I., Fraile-Ardanuy J., Perez J.I., Wilhelmi J.R., Sanchez J.A. (2007). Control of a run of river small hydro power plant. In: *PowerEng2007: International Conference on Power Engineering*, pp. 672.
[6] Borkowski D. (2017). Water level control of a small hydropower plant with a surge tank. *J. Hydraul. Res.* **55**(2), pp. 284-291.
[7] Vesipa R., Ridolfi L. (2019). Overshoots in the water-level control of hydropower plants. *Renewable Energy* **131**, pp. 800-810.
[8] Wang, B., Liu, J., & Wang, C. (2019). Measurement and analysis of backlash on harmonic drive. *Materials Science and Engineering*, **542**, pp. 12005.
[9] Chaudhry, M. H. (1979). *Applied Hydraulic Transients.* New York: Van Nostrand Reinhold.
[10] Devore, J.L. (2012). *Probability & Statistics for Engineering and the Sciences.* Boston: Cengage.
[11] Norconsult SA. (2016). *Svenska kraftnät.* Retrieved from Svenska kraftnät SA: https://www.svk.se/en/press-och-nyheter/news/news/nordic-common-project-for-review-of-primary-reserve-requirements--finalized-phase-1/
[12] Filion, Y.R., Karney, B.W.(2002). Extended-period analysis with a transient model. *Journal of Hydraulic Engineering*, **128**(6), pp. 616–624.
[13] Schmid P.J. (2007). Nonmodal stability theory. *Annu. Rev. Fluid Mech*. **39**, pp. 129-162.
[14] Defina, A. (2003). Numerical experiments on bar growth. *Water Resources Research*, **39**(4), pp. ESG21-ESG212.
[15] Brandt, L., Cossu, C., Henningson, D.S., Chomaz, J.-M., Huerre, P. (2006). Numerical studies of streak instability in boundary layers. *Fluid Mechanics and its Applications*, **78**, pp. 121-126.
[16] Selvam, B., Talon, L., Lesshafft, L., Meiburg, E. (2009). Convective/absolute instability in miscible core-annular flow. Part 2. Numerical simulations and nonlinear global modes. *Journal of Fluid Mechanics*, **618**, pp. 323-348.
[17] Tao, J., Le Quéré, P., Xin, S. (2004). Absolute and convective instabilities of natural convection flow in boundary-layer regime.. *Physical Review E - Statistical, Nonlinear, and Soft Matter Physics*, **70**(6), pp. 066311/1-066311/7.
[18] Vesipa, R., Fellini, S. (2019). Instability of the Tank-Level Control System of Water Mains in Mountainous Environments. *Journal of Hydraulic Engineering*, **145**(7).
[19]Wylie, E. B., Streeter, V. L. (1978). *Fluid Transients.* McGraw-Hill.